



Peroxiredoxin 3 Inhibits Acetaminophen-Induced Liver Pyroptosis Through the Regulation of Mitochondrial ROS

Yue Wang^{1,2}, Yan Zhao¹, Zhecheng Wang¹, Ruimin Sun¹, Boyang Zou¹, Ruixi Li¹, Deshun Liu³, Musen Lin⁴, Junjun Zhou¹, Shili Ning³, Xiaofeng Tian^{3*} and Jihong Yao^{1,2*}

¹ Department of Pharmacology, Dalian Medical University, Dalian, China, ² Institute of Integrative Medicine, Dalian Medical University, Dalian, China, ³ Department of General Surgery, The Second Affiliated Hospital of Dalian Medical University, Dalian, China, ⁴ Department of Pharmacy, The Second Affiliated Hospital of Dalian Medical University, Dalian, China

OPEN ACCESS

Edited by:

Charles E. McCall,
Wake Forest Baptist Medical Center,
United States

Reviewed by:

Albrecht Piper,
University Hospital Frankfurt, Germany
Rosa M. Sainz,
University of Oviedo, Spain

*Correspondence:

Jihong Yao
yaojihong65@dmu.edu.cn
Xiaofeng Tian
txfdl@dmu.edu.cn

Specialty section:

This article was submitted to
Inflammation,
a section of the journal
Frontiers in Immunology

Received: 13 January 2021

Accepted: 28 April 2021

Published: 13 May 2021

Citation:

Wang Y, Zhao Y, Wang Z, Sun R,
Zou B, Li R, Liu D, Lin M, Zhou J,
Ning S, Tian X and Yao J (2021)
Peroxiredoxin 3 Inhibits
Acetaminophen-Induced Liver
Pyroptosis Through the Regulation of
Mitochondrial ROS.
Front. Immunol. 12:652782.
doi: 10.3389/fimmu.2021.652782

Pyroptosis is a newly discovered form of cell death. Peroxiredoxin 3 (PRX3) plays a crucial role in scavenging reactive oxygen species (ROS), but its hepatoprotective capacity in acetaminophen (APAP)-induced liver disease remains unclear. The aim of this study was to assess the role of PRX3 in the regulation of pyroptosis during APAP-mediated hepatotoxicity. We demonstrated that pyroptosis occurs in APAP-induced liver injury accompanied by intense oxidative stress and inflammation, and liver specific PRX3 silencing aggravated the initiation of pyroptosis and liver injury after APAP intervention. Notably, excessive mitochondrial ROS (mtROS) was observed to trigger pyroptosis by activating the NLRP3 inflammasome, which was ameliorated by Mito-TEMPO treatment, indicating that the anti-pyroptotic role of PRX3 relies on its powerful ability to regulate mtROS. Overall, PRX3 regulates NLRP3-dependent pyroptosis in APAP-induced liver injury by targeting mitochondrial oxidative stress.

Keywords: PRX3, pyroptosis, mitochondrial ROS (mtROS), NLRP3 inflammasome, APAP

INTRODUCTION

Acetaminophen (APAP) is one of the most commonly used analgesic and antipyretic drugs. The recommended dose is safe and effective, but overdose causes hepatotoxicity and acute liver failure (ALF) in a dose-dependent manner (1). The initial step in APAP-mediated hepatotoxicity is the formation of the highly reactive intermediate metabolite n-acetyl-p-benzoquinone imine (NAPQI). Excessive formation of NAPQI consumes intracellular glutathione, binds to mitochondrial proteins, and impairs mitochondrial respiration, which subsequently gives rise to overwhelming

Abbreviations: APAP, acetaminophen; DILI, drug-induced liver injury; PRX3, peroxiredoxin 3; ROS, reactive oxygen species; mtROS, mitochondrial ROS; KCs, kupffer cells; ALF, acute liver failure; NAPQI, n-acetyl-p-benzoquinone imine; PCD, programmed cell death; I/R, ischemia/reperfusion; ALT, aminotransferase; AST, aspartic aminotransferase; LDH, lactate dehydrogenase; OD, optical density; H&E, hematoxylin-eosin; IHC, immunohistochemistry; siRNA, small interfering RNA; GSDMD, gasdermin D; GSDMD-N, N-terminal fragment of GSDMD; NAC, n-acetylcysteine; NLRP3, nod-like receptor protein 3; IL-1 β , interleukin-1 beta; IL-18, interleukin-18.

mitochondrial oxidative stress that triggers signaling pathways through mitochondrial toxicity, eventually leading to cell death and sterile inflammation (2, 3). Importantly, the excessive activation of immune cells, such as Kupffer cells (KCs) causes an inability to shut down the persistent activation of the inflammatory response, which results in tissue damage and disease progression (4–7). Recent studies have shown that APAP displays dose-dependent toxicity in primary hepatocytes. Moreover, upon APAP overdose in mice, at least 50% of KCs exhibit a significant loss (8–10). However, the molecular mechanism of liver cell death in APAP-induced hepatotoxic processes needs to be further elucidated.

Pyroptosis is a newly identified type of programmed cell death (PCD) characterized by pore formation in the plasma membrane, swelling, cell rupture, and proinflammatory factor release (11, 12). As early as 1992, Zychlinsky et al. initially observed pyroptosis and described a lytic form of cell death in macrophages infected by *Shigella flexneri* (13). Pyroptosis is related to innate immune activation, participates in sterile inflammation, and contributes to the development of acute and chronic liver disease (14, 15). To date, the relevance of pyroptosis in APAP-mediated liver damage remains enigmatic. It has been suggested that the NLRP3 inflammasome activates pyroptosis in several diseases, including atherosclerosis, Alzheimer's disease, acute kidney and liver diseases (16–21). Reactive oxygen species (ROS) from damaged mitochondria are the main activator of NLRP3, and the mitochondria serve as the docking site for inflammasome assembly (22–24). Nevertheless, there are no studies on the molecular mechanism linking APAP-induced mitochondrial oxidative stress and pyroptosis.

Peroxisomes (PRXs) are a family of thiol peroxidases that scavenge peroxides in cells. Mammals have six PRXs, of which PRX3 is specifically localized in the mitochondria that is the main site for the formation of peroxynitrite and hydrogen peroxide. As the most abundant peroxidase in most mouse tissues, PRX3 not only eliminates a large amount of hydrogen peroxide but also functions as the main target of peroxynitrite in the mitochondria (25, 26). Previous studies have shown that PRX3-knockout mice accumulate relatively high intracellular ROS levels, which increases the severity of LPS-induced lung injury (27). Moreover, PRX3 deficiency accelerates chronic kidney disease by promoting fibrosis and inflammation accompanied by mitochondrial oxidative stress (28). In contrast, PRX3 overexpression in mice protects against traumatic neuronal injury by preserving mitochondrial function and mitochondrial biogenesis (29) and prevents mitochondrial oxidative damage induced by intestinal ischemia/reperfusion (I/R) injury (30). However, the potential role of PRX3 in APAP-induced hepatotoxicity needs to be further clarified. Notably, a proteomic analysis of APAP-induced acute liver injury in mice showed that a decrease in PRX3 levels may be partly responsible for the excessive accumulation of ROS and aldehyde, which impairs mitochondrial structure and function (31). Therefore, determining the role of PRX3 may be helpful in the treatment of APAP-induced hepatotoxicity.

In this study, we hypothesized that pyroptosis participates in APAP-induced liver injury and elucidated the mechanism and

function of PRX3 in this pathological process. These findings may provide new insights and a target for the treatment of APAP overdose.

MATERIALS AND METHODS

Animal Experiments

Male C57BL/6 mice (10 weeks old, specific pathogen-free) were purchased from the Animal Center of Dalian Medical University (Dalian, China). Mice were housed in an environment maintained at $23 \pm 2^\circ\text{C}$ with ad libitum access to food and water under a 12-h light/dark cycle. APAP was purchased from Aladdin (Shanghai, China) and dissolved in warmed 37°C saline. To establish a murine model of APAP-induced ALF, totally 16 male C57BL/6 mice were randomly divided into 2 groups ($n = 8$) and received treatment as follows: a. control group: 24-h-fasted mice were treated with a control agent (normal saline). b. APAP group: 24-h-fasted mice were each given APAP (300 mg/kg) by oral gavage. The mice were sacrificed 12 h after normal saline or APAP gavage, and serum and liver tissues were collected and stored at -80°C for further analysis.

To generate a liver-specific knockdown of PRX3, PRX3-specific small short hairpin RNA (shRNA) was cloned and packaged into an adeno-associated virus 9 (AAV9) with the liver-specific thyroxine binding globulin (TBG) promoter (Hanbio, Shanghai, China). The AAV9-TBG-shRNA-NC/PRX3 was packaged with pAAV-RC and pHelper using the triple-plasmid transient transfection method (HB infusionTM Kit; Hanbio Bio.). Viral particles were applied in the following animal experiments after purification. The shRNA-PRX3 sequence was as follows: 5'-AAGGTATATTGCTGTTGACAGTGAGCGCCAAAGGAAGTCA GCCTTTTAGTGAAGCCACAGATGTAAAAGGCTGACTTTCCTTGGTGCCTACTGCCTCG-3'. In the AAV9-shRNA-treated APAP liver injury model, mice were randomly divided into 4 groups ($n = 8$; totally 32 mice) and administered with 200 μl of AAV9-shRNA-NC/PRX3 (1.9×10^{12} vg/mL) through tail vein injection. At 3 weeks after injection, mice were used in experiments as mentioned before. After the administration of APAP for an additional 12 h, the livers and serum were harvested and analyzed.

All procedures were carried out in accordance with the Institutional Laboratory Animal Care and Use Guidelines and approved by the Institutional Ethics Committee of Dalian Medical University. Animal studies are reported in compliance with the ARRIVE guidelines (32).

Measurement of Serum Parameters

Serum levels of alanine aminotransferase (ALT) and aspartic aminotransferase (AST) were measured with appropriate assay kits (Jiancheng Bioengineering Institute, Nanjing, China).

Enzyme-Linked Immunosorbent Assay

Mice serum levels of IL-1 β and IL-18 were assayed using an enzyme-linked immunosorbent assay (ELISA) kit (Jiancheng

Bioengineering Institute, Nanjing, China) according to the manufacturer's instructions.

Lactate Dehydrogenase Assay

Serum and cellular supernatants were collected for a lactate dehydrogenase (LDH) assay (Jiancheng Bioengineering Institute, Nanjing, China) applied according to the manufacturer's instructions. Optical density (OD) values were measured at 450 nm using a Thermo Multiskan FC microplate photometer.

Histological Examination and Immunohistochemical Staining

Liver tissue sections were cut and fixed with 4% paraformaldehyde at least overnight, and then hematoxylin-eosin (H&E) staining was performed.

Immunohistochemistry (IHC) for PRX3 was performed using 4- μ m-thick paraffin sections. Sections were incubated with an anti-PRX3 antibody (Abcam, Cambridge, UK) overnight at 4°C and then incubated with a secondary antibody (Servicebio, Wuhan, China) at room temperature for 50 min. Subsequently, the tissues were covered with DAB and hematoxylin, and sections were observed via light microscopy.

Isolation and Culture of Primary Liver Cells

Primary KCs and hepatocytes were isolated from mice as described previously (33, 34). Briefly, after 12h fasting, the mice were anesthetized, sterilized with 75% alcohol and fixed on an anatomical plate in the ultra-clean table. 25 mL CMF-HBSS was infused from the hepatic portal vein of mice, and then 25 mL Hank's Balanced Salt Solution (HBSS) with 0.5 mg/ml collagenase IV (both from Solabio, Beijing, China) was infused until the liver failed to rebound after pressing. After digestion, the liver was dissected and placed in a petri dish with a cold HBSS buffer. The cell suspension was successively passed through 100- and 200-mesh filters, and then centrifuged three times at 50 \times g for 3 min to obtain hepatocytes. The initial cell supernatant was collected and centrifuged at 650 \times g at 4°C for 7 min, after which the pelleted cells were resuspended in 2ml HBSS. Then, the cell suspension was gently layered onto an 8ml two-step Percoll gradient (25%/50%; Solabio) in a 15 ml conical centrifuge tube, and the tube was centrifuged at 1800 g for 15 min at 4°C. The intermediate mesophase (white cell ring) was carefully collected, resuspended with HBSS and centrifuged at 650 \times g for 7 min to obtain the precipitated KCs. Isolated primary liver cells were seeded on rat tail collagen I-coated culture plates (Corning Life Sciences, Tewksbury, MA, USA), and the medium was replaced after cell adherence (approximately 3-4h). KCs were maintained in RPMI 1640 medium, and hepatocytes were maintained in DMEM/F12 (both from Gibco, Carlsbad, CA, USA) supplemented with 10% FBS at 37°C under an atmosphere with 5% CO₂. The primary cells were then treated with 10 mM APAP (dissolved in phosphate buffer solution (PBS) at 37°C) for 12 h. All cell treatments were performed in a blinded and random manner.

Western Blotting

All western blotting procedures were performed as previously described (30) with the following primary antibodies: anti-PRX3, anti-NLRP3 (Abclonal Biotechnology, Wuhan, China), anti-

gasdermin D (GSDMD), anti-caspase-1, anti-cleaved caspase-1, anti-IL-1 β (all from Cell Signaling Technology, Boston, MA, USA), anti-IL-18, anti-PRX5 (Abcam, Cambridge, UK), PRX6 (Zen bio., Chengdu, China) and anti- β -actin (Bimake, Houston, TX, USA).

RNA Isolation and qRT-PCR

Total RNA was extracted using TRIzol reagent (Invitrogen, Carlsbad, CA, USA). Then, cDNA synthesis and qRT-PCR were performed with a PrimeScript™ RT reagent kit and SYBR Premix Ex Taq™ II (TaKaRa, Japan), respectively. Specific primers used for qRT-PCR were as follows: mmu-PRX3-FO, (5'-TGCTGGCATTGCACTCAGA-3'), mmu-PRX3-RE (5'-ACTTCTCCATGGGTCTCCACAA-3'), mmu- β -actin-FO (5'-ACTGCCGCATCCTCTTCCT-3'), and mmu- β -actin-RE (5'-TCAACGTCACACTTCATGATGGA-3').

Cell Transfection

Primary cells were isolated from mice liver and seeded into rat tail collagen I-coated culture plates (6-well) at a density of 10⁶ cells per well. The small interfering RNA (siRNA; 50 pM) or negative control (GenePharma, Suzhou, China) was respectively pre-mixed with Lipofectamine™ 3000 Reagent (3.75 μ l per well; Invitrogen, Carlsbad, CA, USA) according to the manufacturer's instructions. After incubating for 15 min at room temperature, the mixtures were added to adherent primary liver cells (approximately 50%) for 36h in the original medium. The PRX3-specific siRNA sequences were sense 5'-CCAAGGAAAG UCAGCCUUTT-3' and antisense 5'-AAAGGCUGAC UUCCUUGGTT-3'. The NLRP3-specific siRNA sequences were sense 5'-CCAACUGGUCAAGGAGCAUTT-3' and antisense 5'-AUGCUCUUGACCAGUUGGTT-3'. The PRX5-specific siRNA sequences were sense 5'-GGCCGGAAAGAAG CAGGUUTT-3' and antisense 5'-AACCUGCUUCUUU CCGGCCTT-3'. The PRX6-specific siRNA sequences were sense 5'-GGACGCUAACAACAUGCCUTT-3' and antisense 5'-AGGCAUGUUGUAGCGUCCTT-3'. The expression plasmid (1 μ g/ml) or negative control plasmid (GenePharma) was respectively pre-mixed with Lipofectamine™ 3000 Reagent (3.75 μ l per well) and P3000™ Reagent (5 μ l per well) for 15 min following the manufacturer's instructions. Then, plasmid DNA-lipid complexes were transfected into adherent primary hepatocytes (approximately 50%) for 48 h in the original medium. After transfection, the cells were incubated with APAP (10 mM) for 12 h for different experiments.

Mitochondrial ROS Level Determination

Mito-TEMPO is a mitochondria-targeted antioxidant, a specific scavenging agent for mitochondrial superoxides. Hepatocytes were stimulated with 200 μ M Mito-TEMPO (dissolved in DMSO) for 1 h, followed by treatment with 10 mM APAP for 12 h.

Mitochondrial ROS levels were detected by visualization with MitoSOX Red (Invitrogen, Carlsbad, CA, USA). Briefly, primary mouse hepatocytes were fixed on a six-well plate and incubated with 5 μ M MitoSOX Red for 10 min at 37°C in the dark. The nuclei were recognized by Hoechst 33342 staining (Beyotime,

Shanghai, China) in the dark for 5-10 min. Immunofluorescence images were obtained under an 80iNikon confocal microscope.

Double Immunofluorescence Microscopy

After fixation in 4% paraformaldehyde, primary hepatocytes were incubated with primary antibody at 4°C overnight, followed by an incubation with secondary antibody (Proteintech, Wuhan, China) at 37°C for 1 h. Subsequently, Hoechst 33342 was used for nuclear staining. Immunofluorescence images were captured with an 80i Nikon confocal microscope.

H₂O₂ Analysis

H₂O₂ levels were examined using a hydrogen peroxide assay kit (Solarbio, Beijing, China) according to the manufacturer's recommended protocol.

Statistical Analysis

All data are presented as the means ± standard deviation (SD). Student's unpaired t-test (two-group comparisons) and one-way ANOVA (multigroup comparisons) were carried out using GraphPad Prism version 7.0 (GraphPad Prism Software, CA, USA). A p-value of < 0.05 was considered to indicate a significant difference.

RESULTS

Pyroptosis Occurs in Mice With APAP-Induced Liver Injury

After excess APAP administration, the serum levels of ALT and AST in mice were clearly elevated (**Figure 1A**). Histological H&E staining revealed that central lobular necrosis, central venous disappearance, and disordered cell arrangement were severe and widespread in the liver of APAP-treated mice (**Figure 1B**). Notably, in the APAP group, the serum LDH content was increased by 6.5-fold compared to that observed in the wild-type mice group (**Figure 1C**), suggesting that a breach in cell membrane integrity and the efflux of cellular contents occurred after APAP stimulation (35). To assess the potential role of pyroptosis in the pathogenesis of APAP-induced hepatotoxicity, we further examined the protein levels of GSDMD, caspase-1, IL-1β, and IL-18, the key proteins in pyroptosis regulation (17, 35, 36). As shown in **Figure 1D**, increased levels of the N-terminal fragment of GSDMD (GSDMD-N) were found in liver tissue of APAP model mice. Similarly, the expression of the precursor of caspase-1 was downregulated, while that of the active fragment of caspase-1 (p20) was significantly upregulated, which resulted in the cleavage and activation of GSDMD. During this period, protein levels and serum levels of the proinflammatory cytokines IL-1β and IL-18 were increased after APAP intervention (**Figures 1E, F**). These results suggest that pyroptosis is related to APAP-induced liver injury.

Primary KCs and Hepatocytes Undergo Pyroptosis Upon APAP Treatment

KCs are rapidly lost after APAP overdose, which is accompanied by inflammatory cell infiltration (9, 10). To investigate whether

pyroptosis contributes to KCs death, we performed western blot analysis of primary KCs exposed to APAP. The results showed that LDH release increased in the supernatants of KCs treated with APAP (**Figure 2A**). Notably, cleaved caspase-1 (p20) expression was dramatically elevated, causing an increase in GSDMD-N levels. Additionally, mature IL-1β and IL-18 levels were upregulated by approximately 2.5- and 2-fold, respectively, in the APAP group compared to the control group (**Figure 2B**). These results suggested that the massive loss of KCs after APAP intervention may have been partly caused by pyroptosis. Furthermore, massive death of hepatocytes is a key event after APAP overdose (8). To verify the association between pyroptosis and hepatocyte death, we assessed LDH and pyroptosis-associated protein levels in primary hepatocytes exposed to APAP. As shown in **Figure 2D**, increased LDH release was detected in APAP-treated hepatocellular supernatants. The precursor protein expression levels of GSDMD, caspase-1, IL-1β and IL-18 were decreased in the APAP group compared to the untreated group, while APAP administration led to substantial upregulation of the levels of the active fragments of these proteins. The dynamic change from the original to the activated forms of these key proteins indicate the occurrence of pyroptosis in primary hepatocytes incubated with APAP (**Figure 2C**).

It is important to note that increasing attention has been paid to the intercellular communication between KCs and hepatocytes (11, 37, 38). After APAP stimulation, we observed that caspase-1 p20 and GSDMD-N levels were upregulated in hepatocytes cocultured with KCs compared to monolayer hepatocytes, with increases in the levels of the inflammatory factors IL-1β and IL-18 also detected (**Figure 2E**). These data suggest that after excessive APAP intake, hepatocytes exposed to KCs underwent more pyroptosis.

PRX3 Silencing Accelerates Pyroptosis in APAP-Induced Hepatotoxicity in Mice

Mitochondrial oxidative stress and intracellular inflammation are generally associated with APAP toxicity (2, 3, 25, 28, 39). To assess the protective effect of the PRX family members on APAP hepatotoxicity, specific siRNAs for three mitochondria-associated PRXs (PRX3, PRX5 and PRX6) (25, 40) were transfected into hepatocytes prior to APAP-induced cytotoxicity (**Figures S1A–C**). As shown in **Figures S1D, E**, we observed that PRX3 silencing resulted in more mtROS and increased inflammatory marker levels (IL-1β and IL-18) compared to knockdown of PRX5 and PRX6 after APAP intervention. These results indicate that PRX3 is a protective target among mitochondria-associated PRXs to prevent APAP-induced hepatotoxicity.

We subsequently evaluated the expression of PRX3 in the livers of mice following APAP administration. As shown in **Figures 3A, B**, PRX3 protein and mRNA levels were significantly decreased after APAP intoxication compared to the control group. To systematically assess the function of PRX3 in APAP-induced liver injury, we generated PRX3 liver-specific knockdown mice by AAV9-shRNA-PRX3 treatment

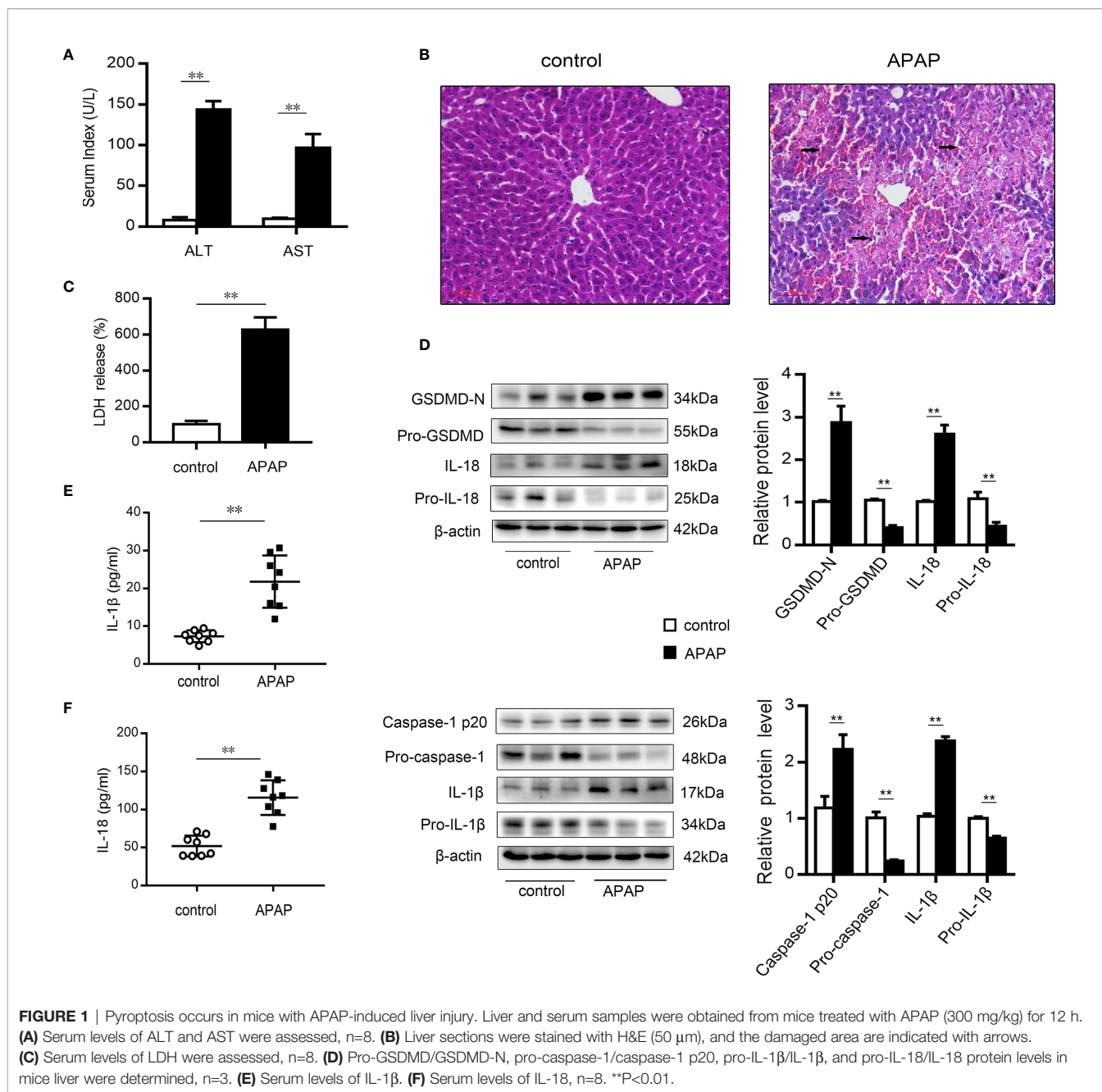
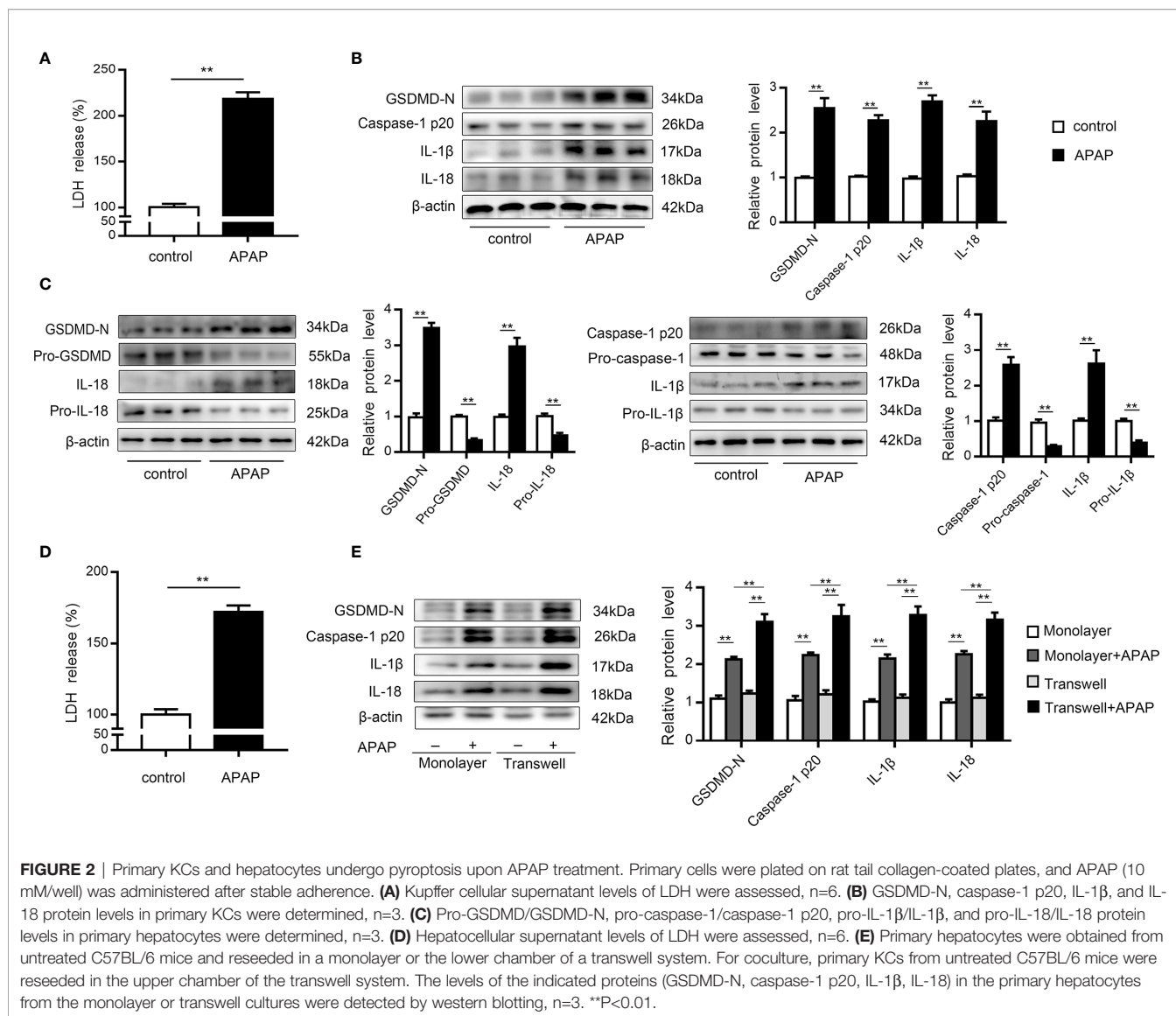


(Figure 3C). IHC and western blotting results indicated that PRX3 expression was notably inhibited by AAV9-shRNA-PRX3 (Figures 3D–J). According to the H&E staining, treatment with PRX3 silencing promoted characteristic centrilobular necrosis after APAP overdose (Figure 3E). Consistent with these results, the serum levels of ALT, AST and LDH release revealed that PRX3 knockdown aggravated APAP-induced liver injury (Figures 3F, G). We further assessed the impact of PRX3 in APAP-induced liver pyroptosis. Liver specific PRX3 silencing markedly increased serum levels of IL-1β and IL-18 as well as liver H₂O₂ levels in mice treated with APAP, indicating fulminant oxidative stress and inflammation (Figures 3H, I, K).

Additionally, as shown in Figure 3J, we observed that AAV9-shRNA-induced PRX3 knockdown significantly upregulated GSDMD, caspase1 p20, IL-1β and IL-18 levels, the specific markers of pyroptosis. Taken together, these results demonstrate that PRX3 is associated with pyroptosis in APAP-induced hepatotoxicity.

PRX3 Regulates NLRP3-Mediated Pyroptosis in APAP-Induced Hepatotoxicity *In Vitro*

We further investigated the underlying mechanisms of APAP-induced liver pyroptosis. NLRP3 inflammasome activation is



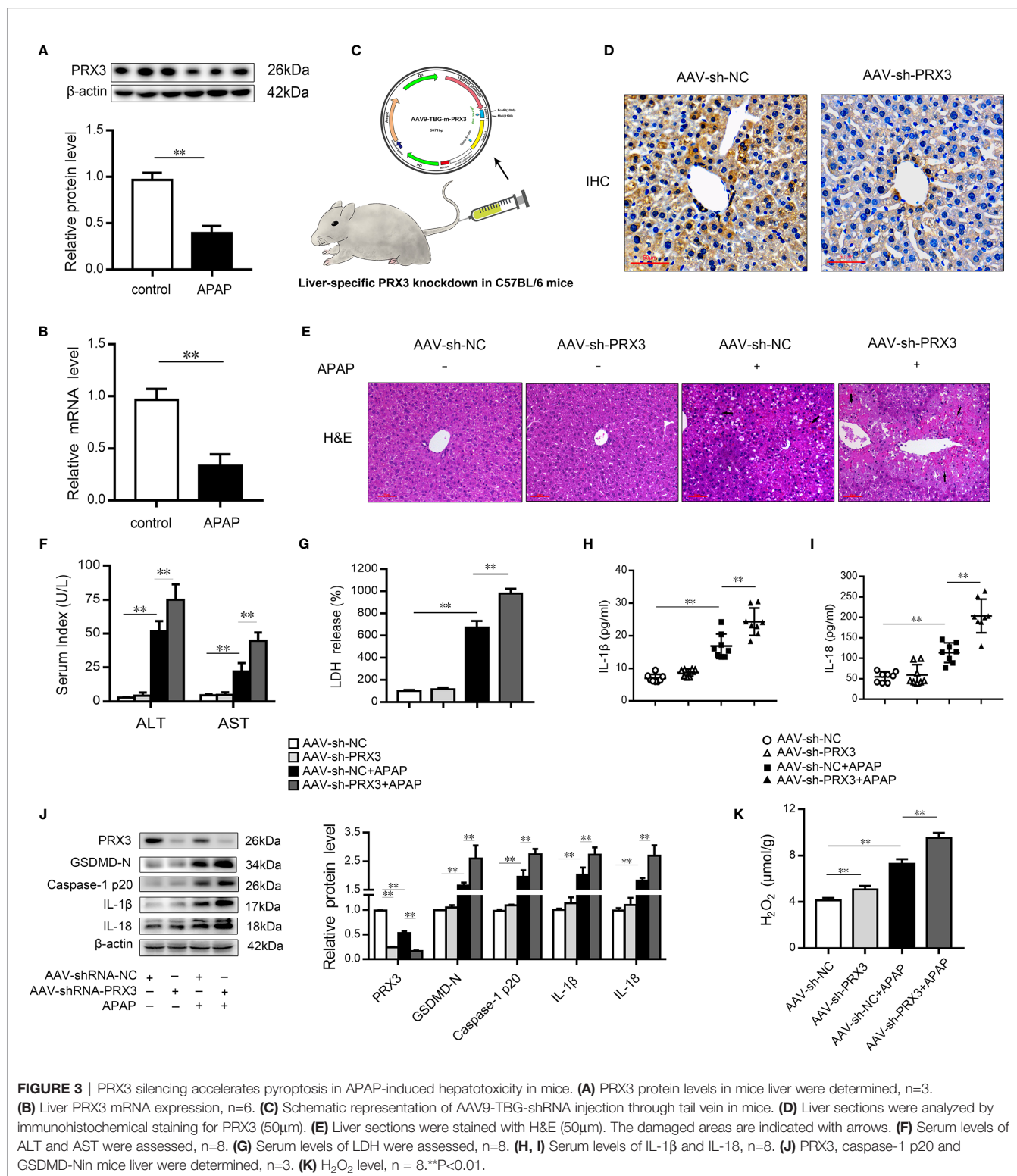
regarded as a major event in the initiation of pyroptosis (16, 23). As shown in **Figure S2A**, NLRP3 expression in mice was markedly increased after APAP treatment. Consistently, we observed the same trend *in vitro* (**Figures S2B, C**). Interestingly, NLRP3-specific siRNAs rescued APAP-induced cell death determined by LDH release in supernatant of KCs and hepatocytes (**Figures 4A, C**). Furthermore, we found that si-NLRP3 resulted in a notable recovery of cleaved GSDMD, caspase-1, IL- β and IL-18 expression induced by APAP treatment (**Figures 4B, D**). Thus, NLRP3 contributes to the pathogenesis of APAP-induced liver pyroptosis.

In primary KCs and hepatocytes exposed to APAP, PRX3 protein levels showed the same downward tendency (**Figures S2D, E**). To further assess whether PRX3 plays a role in NLRP3-dependent pyroptosis *in vitro*, hepatocytes were transfected with PRX3-specific pcDNA or siRNA prior to APAP intoxication. Double immunofluorescence staining confirmed that PRX3 (green) and NLRP3 (red) were both located in the

mitochondria and highly colocalized (**Figure 4H**). Notably, overexpression of PRX3 reduced the activation-responsive protein expression of pyroptotic genes, impaired NLRP3 inflammasome activation and inhibited LDH release (**Figures 4E–G**), while knockdown of PRX3 significantly enhanced NLRP3 inflammasome activation and stimulated pyroptosis (**Figures 4I–K**). Thus, our data indicate that PRX3 regulates APAP-associated pyroptosis through the NLRP3 inflammasome.

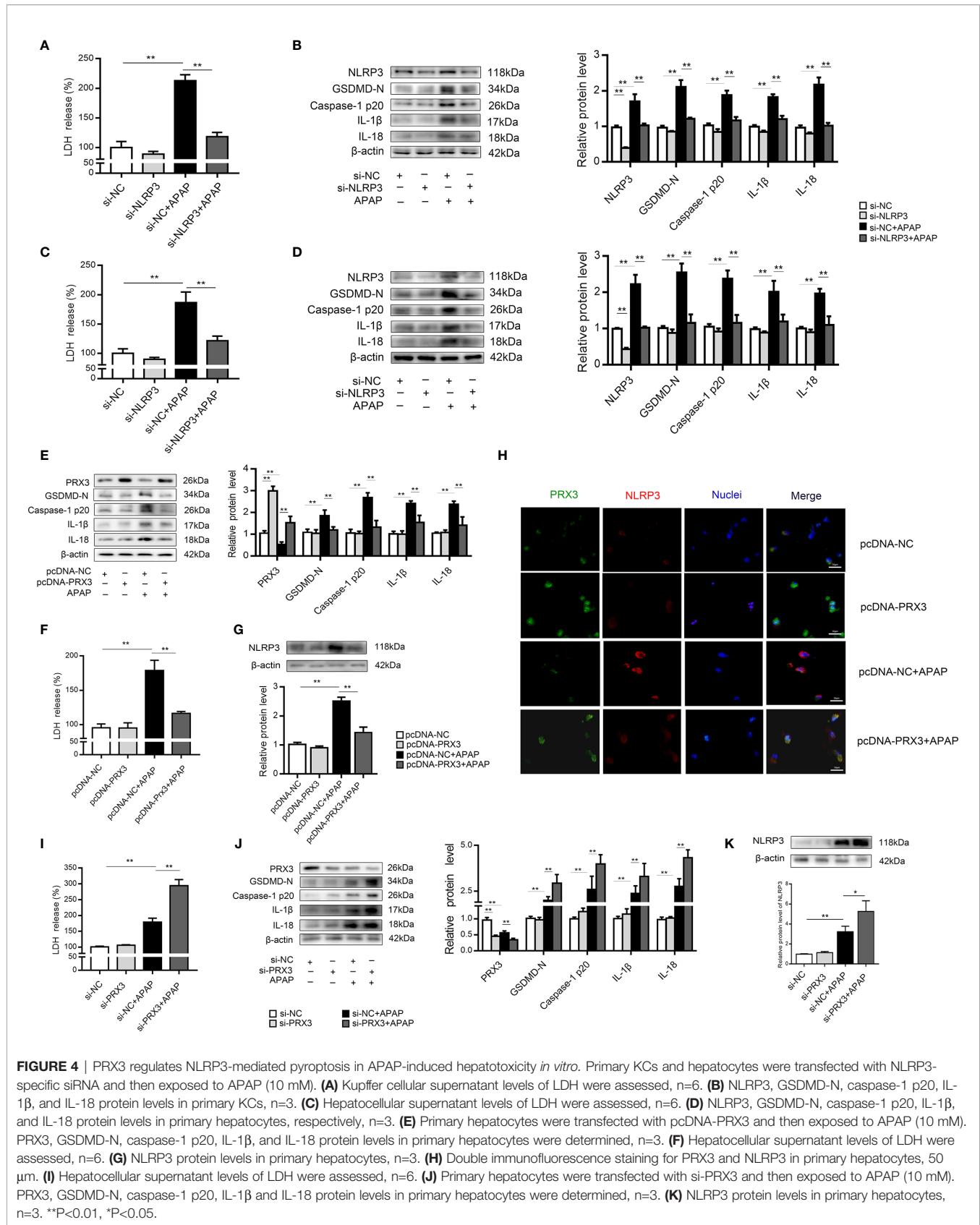
PRX3 Regulates the NLRP3 Inflammasome Through Mitochondrial ROS After APAP Overdose

To further investigate the regulatory mechanism between PRX3 and NLRP3, KCs and hepatocytes were co-transfected with PRX3- and NLRP3-specific siRNAs prior to APAP overdose. As shown in **Figures 5A, B**, PRX3 knockdown aggravated the triggering effect of NLRP3 on pyroptosis (including the increased serum level of LDH and protein levels of GSDMD-N, caspase-1



p20, IL-1β and IL-18) in KCs, which was vastly attenuated by NLRP3-specific siRNA. Additionally, we observed the same results in hepatocytes (**Figures 5C, D**). Taken together, our results suggest that PRX3 is a crucial upstream mediator of NLRP3 in the regulation of pyroptosis.

Mitochondrial ROS play a vital role in NLRP3 inflammasome activation (22), and ROS can be inhibited by PRX3 through its antioxidant function (28). To further investigate the relationship between PRX3 and NLRP3, we transfected hepatocytes with PRX3-specific siRNA in the absence/presence of Mito-TEMPO



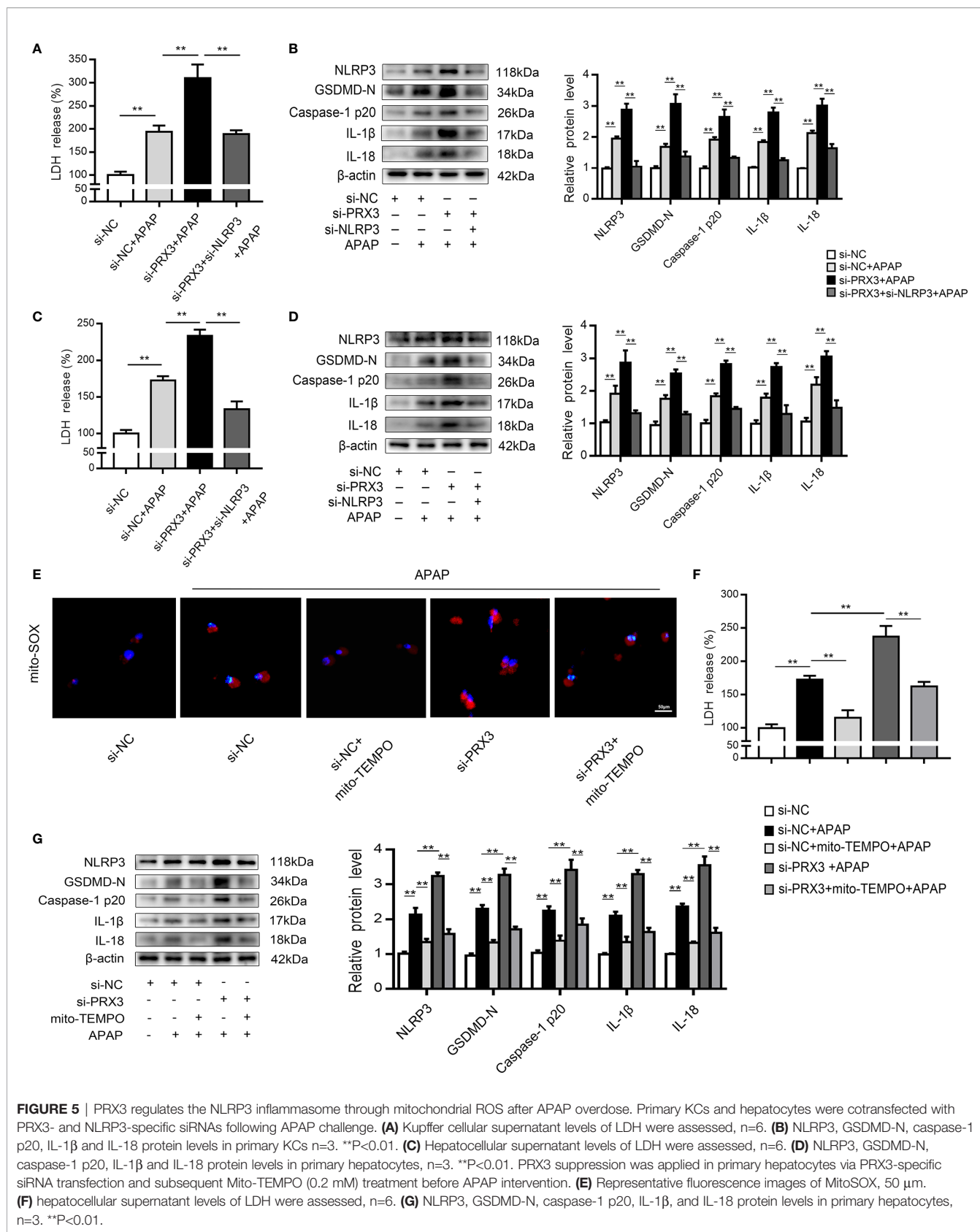


FIGURE 5 | PRX3 regulates the NLRP3 inflammasome through mitochondrial ROS after APAP overdose. Primary KCs and hepatocytes were cotransfected with PRX3- and NLRP3-specific siRNAs following APAP challenge. **(A)** Kupffer cellular supernatant levels of LDH were assessed, n=6. **(B)** NLRP3, GSDMD-N, caspase-1 p20, IL-1 β and IL-18 protein levels in primary KCs n=3. **P<0.01. **(C)** Hepatocellular supernatant levels of LDH were assessed, n=6. **(D)** NLRP3, GSDMD-N, caspase-1 p20, IL-1 β and IL-18 protein levels in primary hepatocytes, n=3. **P<0.01. PRX3 suppression was applied in primary hepatocytes via PRX3-specific siRNA transfection and subsequent Mito-TEMPO (0.2 mM) treatment before APAP intervention. **(E)** Representative fluorescence images of MitoSOX, 50 μ m. **(F)** hepatocellular supernatant levels of LDH were assessed, n=6. **(G)** NLRP3, GSDMD-N, caspase-1 p20, IL-1 β , and IL-18 protein levels in primary hepatocytes, n=3. **P<0.01.

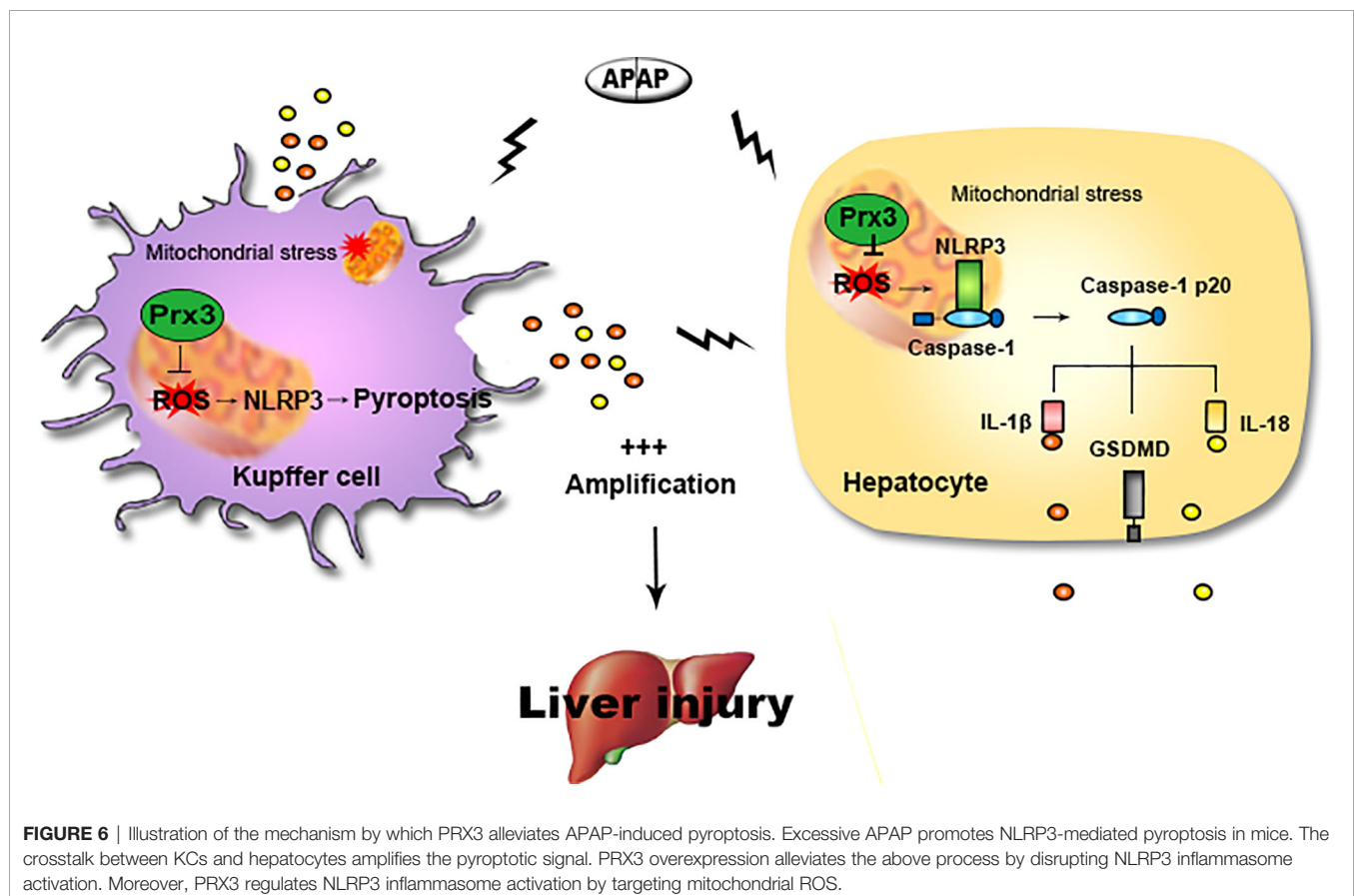
(a specific mtROS scavenger). Under APAP stimulation, PRX3 knockdown resulted in abundant mtROS production in hepatocytes, which was blocked by Mito-TEMPO, as detected using Mito-SOX (Figure 5E). Furthermore, the decreased mtROS levels resulting from Mito-TEMPO treatment substantially attenuated the activation of NLRP3, caspase-1 and GSDMD, as well as the secretion of IL-1 β , IL-18 and LDH (Figures 5F, G). Considering all of the above data, these results suggest that the effect of PRX3 on NLRP3 activation in APAP-induced liver pyroptosis is potentially mediated by mtROS.

DISCUSSION

The main findings of this study are as follows: (1) NLRP3-mediated pyroptosis contributes to APAP-mediated liver injury, while cellular crosstalk between KCs and hepatocytes amplifies the signal for pyroptosis; (2) PRX3 silencing aggravates APAP-induced liver pyroptosis and injury *in vivo* and *in vitro*; (3) PRX3 confers protection against APAP-induced pyroptosis by inhibiting NLRP3 inflammasome activation; and (4) PRX3 regulates the NLRP3 inflammasome by targeting mitochondrial ROS (Figure 6). These findings suggest that PRX3 may be a new therapeutic target in pyroptosis in the context of APAP-induced acute liver injury.

APAP-induced hepatotoxicity is a leading cause of hepatic failure involving multiple intracellular events, including

mitochondrial damage, oxidative stress, and inflammation (41). Especially, secondary multiorgan failure, which is caused by APAP toxicity, is often a result of the initial massive proinflammatory response and generates a systemic inflammatory response syndrome (42). As an inherently inflammatory process, pyroptosis plays vital roles in cellular lysis and proinflammatory cytokine release when hosts defend against infections (43). However, pyroptosis has not been clearly described in APAP-induced liver injury (14). The viewpoint of pyroptosis in APAP poisoning was controversial, possibly because Imaeda (44) and Williams (45) held opposite views on the role of NLRP3 and caspase-1 in APAP-induced liver injury. Thus, additional evidence is needed to investigate whether pyroptosis is involved in APAP hepatotoxicity. In the present study, we observed that upregulation of LDH release occurred concurrently with liver damage, which suggests that cellular damage occurs after APAP stimulation. More importantly, the levels of the active fragments of pyroptosis-related proteins (GSDMD-N, caspase-1 p20, IL-1 β and IL-18) greatly increased upon APAP exposure *in vivo* and *in vitro*. Pyroptosis is induced by the plasma membrane insertion of large pre-assembled non-selective GSDMD-N pores that allowed IL-1 β and IL-18 to be released into the blood, giving rise to rapid cellular swelling and lysis (46). Indeed, we observed that APAP overdose gave rise to a massive release of IL-1 β and IL-18 into the serum of mice by ELISA. In addition, when exposed to KCs, hepatocytes underwent much more pyroptosis after APAP intervention, which is consistent with the



view of Li Y Z et al. (47). Therefore, pyroptosis is closely associated with APAP-induced liver injury.

PRX3 is primarily located in the mitochondria and plays crucial roles in the reduction and clearance of H₂O₂ and peroxynitrite (26). Recent studies have demonstrated that PRX3 knockdown increases mitochondrial superoxide levels (48) and induces the activation of RAW264.7 macrophages (28). Furthermore, relatively high levels of ROS and TNF- α accumulation have been detected in PRX3-deficient peritoneal macrophages (49), indicating that PRX3 is associated with inflammation. Notably, we observed that pyroptosis was involved in APAP-induced hepatotoxicity, and was accompanied by increasing levels of inflammatory factor. In light of these studies, we hypothesized that the antioxidative capacity of PRX3 is associated with the regulation of pyroptosis. Interestingly, our results demonstrated that PRX3 levels decreased upon APAP challenge. Additionally, upon APAP intoxication, PRX3 silencing aggravated liver pyroptosis and injury compared to the control group *in vivo* and *in vitro*. In contrast, enhanced levels of pyroptotic markers stimulated by APAP overdose were reversed by PRX3 overexpression *in vitro*. Hence, PRX3 regulates APAP-induced liver pyroptosis.

We further investigated the mechanism by which PRX3 regulates APAP-induced pyroptosis by assessing NLRP3 inflammasome activation, which has been revealed by increasing evidence to be a key promoter of pyroptosis in several diseases (18–21). Our results confirmed that NLRP3 knockdown led to the suppression of pyroptosis during APAP-induced hepatotoxicity *in vitro*. Mitochondria have been reported to act as docking sites for NLRP3 inflammasome assembly (23) and our subsequent observations revealed that PRX3 colocalized with NLRP3 in the mitochondria. Moreover, PRX3 overexpression was shown to impair NLRP3 inflammasome activation upon exposure to APAP, while PRX3 knockdown enhanced NLRP3 inflammasome activation. Moreover, our data showed that pyroptosis caused by PRX3 deficiency was antagonized by NLRP3-specific siRNA. Collectively, these results confirm that PRX3 may be responsible for modulating the NLRP3 inflammasome and, ultimately, for the initiation of pyroptosis. Excessive mitochondrial ROS promotes the initiation of NLRP3 inflammasome activation (50). After APAP overdose, we observed that the treatment of primary hepatocytes with Mito-TEMPO blocked the PRX3 knockdown-induced release of mitochondrial ROS and the high NLRP3 expression, which simultaneously resulted in the decreased expression of pyroptosis-associated proteins. These results indicate that the anti-pyroptotic effect of PRX3 in the context of APAP-induced hepatotoxicity is associated with suppression of NLRP3 inflammasome activation and is mediated by inhibiting mitochondrial oxidative stress.

Our findings demonstrate that oxidative stress and pyroptosis are not independent but rather interact to facilitate the complexity of APAP-induced liver injury, which is partly consistent with the view of Diao (51). PRX3 plays a major role in mitochondrial redox signaling (25) and is a crucial factor in various diseases, such as colon cancer, chronic hyperglycemia and hepatocellular carcinoma (52–54). In the present study, for the first time, we demonstrated that PRX3 overexpression

mitigates APAP-induced liver pyroptosis, although this alleviation may occur through other pathological processes, which needs to be further investigated. At present, N-acetylcysteine (NAC) is the only currently approved antidote for APAP overdose. Unfortunately, fairly high doses and prolonged treatment times are required due to the poor bioavailability of NAC and the associated anaphylactoid reactions (55, 56). Therefore, the development of therapeutic strategies to regulate PRX3 function may represent a more effective alternative to combat APAP-induced hepatotoxicity. The considerable potential of human Prx3 (hPrx3) as a tecton for use in protein nanotechnology has been previously demonstrated. hPrx3 forms toroidal oligomers characteristic of the PRX family and shows an amazing array of supramolecular assemblies (57), indicating the potential use of PRX3 in the development of specific and novel drugs to treat liver injury.

In summary, the results of our present study demonstrated for the first time, that PRX3 inhibits APAP-induced pyroptosis by inhibiting NLRP3 activation, which depends on the increase in mitochondrial ROS levels. These findings identify the crucial regulatory role of PRX3 in APAP-induced liver damage and provides novel insights into the pathological mechanisms of APAP-induced liver injury.

DATA AVAILABILITY STATEMENT

The original contributions presented in the study are included in the article/**Supplementary Material**. Further inquiries can be directed to the corresponding authors.

ETHICS STATEMENT

The animal study was reviewed and approved by The Institutional Ethics Committee of Dalian Medical University.

AUTHOR CONTRIBUTIONS

JY, XT, and YW designed the study. YW, YZ, ZW, DL, and RS performed the experiments. ML, BZ, and RL analyzed the data. YW, JZ, and SN contributed experimental materials. JY, XT, and YW prepared the manuscript. JY, YZ, ML, and SN provided financial support. All authors contributed to the article and approved the submitted version.

FUNDING

This study was funded by the National Natural Science Foundation of China (Nos. 81973381, 81773799, 82004044 and 81903900), Liaoning Provincial Natural Science Foundation of China (Nos. 20180551172), and Dalian Medical Science Research (Nos. 1712044).

SUPPLEMENTARY MATERIAL

The Supplementary Material for this article can be found online at: <https://www.frontiersin.org/articles/10.3389/fimmu.2021.652782/full#supplementary-material>

Supplementary Figure 1 | Primary hepatocytes were transfected with specific siRNAs of PRX3, PRX5 and PRX6 prior to APAP-induced cytotoxicity. **(A–C)** PRX3,

PRX5 and PRX6 knockdown levels in primary hepatocytes, n=3. **P<0.01 **(D)** IL-1 β and IL-18 protein levels in primary hepatocytes, n=3. **P <0.01 vs. si-NC group. ns, #P <0.05 and ##P <0.01 vs. si-NC + APAP group. **(E)** Representative fluorescence images of MitoSOX (50 μ m).

Supplementary Figure 2 | **(A)** NLRP3 protein levels in mice liver, n=3. **(B)** NLRP3 protein levels in primary KCs, n=3. **(C)** NLRP3 protein levels in primary hepatocytes, n=3. **(D)** PRX3 protein levels in primary KCs were determined, n=3. **(E)** PRX3 protein levels in primary hepatocytes were determined, n=3. **P<0.01.

REFERENCES

- Yan M, Huo Y, Yin S, Hu H. Mechanisms of Acetaminophen-Induced Liver Injury and its Implications for Therapeutic Interventions. *Redox Biol* (2018) 17:274–83. doi: 10.1016/j.redox.2018.04.019
- Du K, Ramachandran A, Jaeschke H. Oxidative Stress During Acetaminophen Hepatotoxicity: Sources, Pathophysiological Role and Therapeutic Potential. *Redox Biol* (2016) 10:148–56. doi: 10.1016/j.redox.2016.10.001
- Woolbright BL, Jaeschke H. Role of the Inflammasome in Acetaminophen-Induced Liver Injury and Acute Liver Failure. *J Hepatol* (2017) 66(4):836–48. doi: 10.1016/j.jhep.2016.11.017
- Yamada N, Karasawa T, Kimura H, Watanabe S, Komada T, Kamata R, et al. Ferroptosis Driven by Radical Oxidation of N-6 Polyunsaturated Fatty Acids Mediates Acetaminophen-Induced Acute Liver Failure. *Cell Death Dis* (2020) 11(2):144. doi: 10.1038/s41419-020-2334-2
- Woolbright BL, Jaeschke H. Mechanisms of Inflammatory Liver Injury and Drug-Induced Hepatotoxicity. *Curr Pharmacol Rep* (2018) 4(5):346–57. doi: 10.1007/s40495-018-0147-0
- Yang R, Tennesseer TL. Damps and Sterile Inflammation in Drug Hepatotoxicity. *Hepatol Int* (2019) 13(1):42–50. doi: 10.1007/s12072-018-9911-9
- Wree A, Holtmann TM, Inzaugarat ME, Feldstein AE. Novel Drivers of the Inflammatory Response in Liver Injury and Fibrosis. *Semin Liver Dis* (2019) 39(3):275–82. doi: 10.1055/s-0039-1685515
- Li Z, Weinman SA. Regulation of Hepatic Inflammation Via Macrophage Cell Death. *Semin Liver Dis* (2018) 38(4):340–50. doi: 10.1055/s-0038-1670674
- Mossanen JC, Krenkel O, Ergen C, Govaere O, Liepelt A, Puengel T, et al. Chemokine (C-C Motif) Receptor 2-Positive Monocytes Aggravate the Early Phase of Acetaminophen-Induced Acute Liver Injury. *Hepatology* (2016) 64(5):1667–82. doi: 10.1002/hep.28682
- Zigmond E, Samia-Grinberg S, Pasmanik-Chor M, Brazowski E, Shibolet O, Halpern Z, et al. Infiltrating Monocyte-Derived Macrophages and Resident Kupffer Cells Display Different Ontogeny and Functions in Acute Liver Injury. *J Immunol* (2014) 193(1):344–53. doi: 10.4049/jimmunol.1400574
- Wang X, Chang CH, Jiang J, Liu X, Li J, Liu Q, et al. Mechanistic Differences in Cell Death Responses to Metal-Based Engineered Nanomaterials in Kupffer Cells and Hepatocytes. *Small* (2020) 16(21):e2000528. doi: 10.1002/smll.202000528
- Gautheron J, Gores GJ, Rodrigues CMP. Lytic Cell Death in Metabolic Liver Disease. *J Hepatol* (2020) 73(2):394–408. doi: 10.1016/j.jhep.2020.04.001
- Zychlinsky A, Prevost MC, Sansonetti PJ. Shigella Flexneri Induces Apoptosis in Infected Macrophages. *Nature* (1992) 358(6382):167–9. doi: 10.1038/358167a0
- Iorga A, Dara L. Cell Death in Drug-Induced Liver Injury. *Adv Pharmacol* (2019) 85:31–74. doi: 10.1016/bs.apha.2019.01.006
- Wu J, Lin S, Wan B, Velani B, Zhu Y. Pyroptosis in Liver Disease: New Insights Into Disease Mechanisms. *Aging Dis* (2019) 10(5):1094–108. doi: 10.14336/AD.2019.0116
- Gaul S, Leszczynska A, Alegre F, Kaufmann B, Johnson CD, Adams LA, et al. Hepatocyte Pyroptosis and Release of Inflammasome Particles Induce Stellate Cell Activation and Liver Fibrosis. *J Hepatol* (2021) 74(1):156–67. doi: 10.1016/j.jhep.2020.07.041
- VVanaja SK, Rathinam VA, Fitzgerald KA. Mechanisms of Inflammasome Activation: Recent Advances and Novel Insights. *Trends Cell Biol* (2015) 25(5):308–15. doi: 10.1016/j.tcb.2014.12.009
- Wu Q, He X, Wu LM, Zhang RY, Li LM, Wu CM, et al. Mkl1 Aggravates Ox-Ldl-Induced Cell Pyroptosis Via Activation of NLRP3 Inflammasome in Human Umbilical Vein Endothelial Cells. *Inflammation* (2020) 43(6):2222–31. doi: 10.1007/s10753-020-01289-8
- Chen DB, Gao HW, Peng C, Pei SQ, Dai AR, Yu XT, et al. Quinones as Preventive Agents in Alzheimer's Diseases: Focus on NLRP3 Inflammasomes. *J Pharm Pharmacol* (2020) 72(11):1481–90. doi: 10.1111/jphp.13332
- Tan J, Fan J, He J, Zhao L, Tang H. Knockdown of LncRNA DLX6-AS1 Inhibits HK-2 Cell Pyroptosis Via Regulating miR-223-3p/NLRP3 Pathway in Lipopolysaccharide-Induced Acute Kidney Injury. *J Bioenerg Biomembr* (2020) 52(5):367–76. doi: 10.1007/s10863-020-09845-5
- Shi C, Wang Q, Rao Z, Shi Y, Wei S, Wang H, et al. Diabetes Induces Hepatocyte Pyroptosis by Promoting Oxidative Stress-Mediated NLRP3 Inflammasome Activation During Liver Ischaemia and Reperfusion Injury. *Ann Transl Med* (2020) 8(12):739. doi: 10.21037/atm-20-1839
- Shan S, Shen Z, Zhang C, Kou R, Xie K, Song F. Mitophagy Protects Against Acetaminophen-Induced Acute Liver Injury in Mice Through Inhibiting NLRP3 Inflammasome Activation. *Biochem Pharmacol* (2019) 169:113643. doi: 10.1016/j.bcp.2019.113643
- Swanson KV, Deng M, Ting JP. The NLRP3 Inflammasome: Molecular Activation and Regulation to Therapeutics. *Nat Rev Immunol* (2019) 19(8):477–89. doi: 10.1038/s41577-019-0165-0
- Abais JM, Xia M, Zhang Y, Boini KM, Li PL. Redox Regulation of NLRP3 Inflammasomes: ROS as Trigger or Effector? *Antioxid Redox Signal* (2015) 22(13):1111–29. doi: 10.1089/ars.2014.5994
- Cox AG, Winterbourn CC, Hampton MB. Mitochondrial Peroxiredoxin Involvement in Antioxidant Defence and Redox Signalling. *Biochem J* (2009) 425(2):313–25. doi: 10.1042/BJ20091541
- De Armas MI, Esteves R, Viera N, Reyes AM, Mastrogianni M, Alegria TGP, et al. Rapid Peroxynitrite Reduction by Human Peroxiredoxin 3: Implications for the Fate of Oxidants in Mitochondria. *Free Radic Biol Med* (2019) 130:369–78. doi: 10.1016/j.freeradbiomed.2018.10.451
- Li L, Shoji W, Takano H, Nishimura N, Aoki Y, Takahashi R, et al. Increased Susceptibility of MER5 (Peroxiredoxin III) Knockout Mice to LPS-induced Oxidative Stress. *Biochem Biophys Res Commun* (2007) 355(3):715–21. doi: 10.1016/j.bbrc.2007.02.022
- Hwang I, Uddin MJ, Lee G, Jiang S, Pak ES, Ha H. Peroxiredoxin 3 Deficiency Accelerates Chronic Kidney Injury in Mice Through Interactions Between Macrophages and Tubular Epithelial Cells. *Free Radic Biol Med* (2019) 131:162–72. doi: 10.1016/j.freeradbiomed.2018.12.002
- Hu W, Dang XB, Wang G, Li S, Zhang YL. Peroxiredoxin-3 Attenuates Traumatic Neuronal Injury Through Preservation of Mitochondrial Function. *Neurochem Int* (2018) 114:120–6. doi: 10.1016/j.neuint.2018.02.004
- Wang Z, Sun R, Wang G, Chen Z, Li Y, Zhao Y, et al. SIRT3-Mediated Deacetylation of PRDX3 Alleviates Mitochondrial Oxidative Damage and Apoptosis Induced by Intestinal Ischemia/Reperfusion Injury. *Redox Biol* (2020) 28:101343. doi: 10.1016/j.redox.2019.101343
- Feng Q, Zhao N, Xia W, Liang C, Dai G, Yang J, et al. Integrative Proteomics and Immunochromatography Analysis of the Factors in the Necrosis and Repair in Acetaminophen-Induced Acute Liver Injury in Mice. *J Cell Physiol* (2019) 234(5):6561–81. doi: 10.1002/jcp.27397
- Kilkenny C, Browne W, Cuthill IC, Emerson M, Altman DG. Nc3rs Reporting Guidelines Working Group. Animal Research: Reporting In Vivo Experiments: The ARRIVE Guidelines. *Br J Pharmacol* (2010) 160(7):1577–9. doi: 10.1111/j.1476-5381.2010.00872.x

33. Aparicio-Vergara M, Tencerova M, Morgantini C, Barreby E, Aouadi M. Isolation of Kupffer Cells and Hepatocytes From a Single Mouse Liver. *Methods Mol Biol* (2017) 1639:161–71. doi: 10.1007/978-1-4939-7163-3_16
34. Wang Q, Ou Y, Hu G, Wen C, Yue S, Chen C, et al. Naringenin Attenuates non-Alcoholic Fatty Liver Disease by Down-Regulating the NLRP3/NF- κ B Pathway in Mice. *Br J Pharmacol* (2020) 177(8):1806–21. doi: 10.1111/bph.14938
35. Lan P, Fan Y, Zhao Y, Lou X, Monsour HP, Zhang X, et al. TNF Superfamily Receptor OX40 Triggers Invariant NKT Cell Pyroptosis and Liver Injury. *J Clin Invest* (2017) 127(6):2222–34. doi: 10.1172/JCI91075
36. Zhang X, Luan J, Chen W, Fan J, Nan Y, Wang Y, et al. Mesoporous Silica Nanoparticles Induced Hepatotoxicity Via NLRP3 Inflammasome Activation and caspase-1-dependent Pyroptosis. *Nanoscale* (2018) 10(19):9141–52. doi: 10.1039/c8nr00554k
37. Laskin DL, Pilaro AM, Ji S. Potential Role of Activated Macrophages in Acetaminophen Hepatotoxicity. II. Mechanism of Macrophage Accumulation and Activation. *Toxicol Appl Pharmacol* (1986) 86(2):216–26. doi: 10.1016/0041-008x(86)90052-9
38. West MA, Keller GA, Hyland BJ, Cerra FB, Simmons RL. Hepatocyte Function in Sepsis: Kupffer Cells Mediate a Biphasic Protein Synthesis Response in Hepatocytes After Exposure to Endotoxin or Killed *Escherichia Coli*. *Surgery* (1985) 98(3):388–95.
39. Wang X, Wu Q, Liu A, Anadón A, Rodríguez JL, Martínez-Larrañaga MR, et al. Paracetamol: Overdose-Induced Oxidative Stress Toxicity, Metabolism, and Protective Effects of Various Compounds In Vivo and In Vitro. *Drug Metab Rev* (2017) 49(4):395–437. doi: 10.1080/03602532.2017.1354014
40. Ma S, Zhang X, Zheng L, Li Z, Zhao X, Lai W, et al. Peroxiredoxin 6 Is a Crucial Factor in the Initial Step of Mitochondrial Clearance and Is Upstream of the PINK1-Parkin Pathway. *Antioxid Redox Signal* (2016) 24(9):486–501. doi: 10.1089/ars.2015.6336
41. Viswanathan P, Sharma Y, Gupta P, Gupta S. Replicative Stress and Alterations in Cell Cycle Checkpoint Controls Following Acetaminophen Hepatotoxicity Restrict Liver Regeneration. *Cell Prolif* (2018) 51(3):e12445. doi: 10.1111/cpr.12445
42. Dong V, Nanchal R, Karvellas CJ. Pathophysiology of Acute Liver Failure. *Nutr Clin Pract* (2020) 35(1):24–9. doi: 10.1002/ncp.10459
43. Guo H, Xie M, Zhou C, Zheng M. The Relevance of Pyroptosis in the Pathogenesis of Liver Diseases. *Life Sci* (2019) 223:69–73. doi: 10.1016/j.lfs.2019.02.060
44. Imaeda AB, Watanabe A, Sohail MA, Mahmood S, Mohamadnejad M, Sutterwala FS, et al. Acetaminophen-Induced Hepatotoxicity in Mice is Dependent on Tlr9 and the Nalp3 Inflammasome. *J Clin Invest* (2009) 119(2):305–14. doi: 10.1172/JCI35958
45. Williams CD, Antoine DJ, Shaw PJ, Benson C, Farhood A, Williams DP, et al. Role of the Nalp3 Inflammasome in Acetaminophen-Induced Sterile Inflammation and Liver Injury. *Toxicol Appl Pharmacol* (2011) 252(3):289–97. doi: 10.1016/j.taap.2011.03.001
46. de Vasconcelos NM, Van Opdenbosch N, Van Gorp H, Parthoens E, Lamkanfi M. Single-Cell Analysis of Pyroptosis Dynamics Reveals Conserved GSDMD-mediated Subcellular Events That Precede Plasma Membrane Rupture. *Cell Death Differ* (2019) 26(1):146–61. doi: 10.1038/s41418-018-0106-7
47. Zhang LY, Zhan DL, Chen YY, Wang WH, He CY, Lin Y, et al. Aflatoxin B1 Enhances Pyroptosis of Hepatocytes and Activation of Kupffer Cells to Promote Liver Inflammatory Injury Via Dephosphorylation of cyclooxygenase-2: An In Vitro, Ex Vivo and In Vivo Study. *Arch Toxicol* (2019) 93(11):3305–20. doi: 10.1007/s00204-019-02572-w
48. Huh JY, Kim Y, Jeong J, Park J, Kim I, Huh KH, et al. Peroxiredoxin 3 is a Key Molecule Regulating Adipocyte Oxidative Stress, Mitochondrial Biogenesis, and Adipokine Expression. *Antioxid Redox Signal* (2012) 16(3):229–43. doi: 10.1089/ars.2010.3766
49. Li L, Kaifu T, Obinata M, Takai T. Peroxiredoxin III-deficiency Sensitizes Macrophages to Oxidative Stress. *J Biochem* (2009) 145(4):425–7. doi: 10.1093/jb/mvp011
50. Kelley N, Jeltema D, Duan Y, He Y. The NLRP3 Inflammasome: An Overview of Mechanisms of Activation and Regulation. *Int J Mol Sci* (2019) 20(13):3328. doi: 10.3390/ijms20133328
51. Diao C, Chen Z, Qiu T, Liu H, Yang Y, Liu X, et al. Inhibition of PRMT5 Attenuates Oxidative Stress-Induced Pyroptosis Via Activation of the Nrf2/HO-1 Signal Pathway in a Mouse Model of Renal Ischemia-Reperfusion Injury. *Oxid Med Cell Longev* (2019) 25:2345658. doi: 10.1155/2019/2345658
52. Song IS, Jeong YJ, Jeong SH, Heo HJ, Kim HK, Bae KB, et al. Foxm1-Induced PRX3 Regulates Stemness and Survival of Colon Cancer Cells Via Maintenance of Mitochondrial Function. *Gastroenterology* (2015) 149(4):1006–16. doi: 10.1053/j.gastro.2015.06.007
53. Elumalai S, Karunakaran U, Moon JS, Won KC. High Glucose-Induced PRDX3 Acetylation Contributes to Glucotoxicity in Pancreatic β -Cells: Prevention by Teneligliptin. *Free Radic Biol Med* (2020) 160:618–29. doi: 10.1016/j.freeradbiomed.2020.07.030
54. Qiao B, Wang J, Xie J, Niu Y, Ye S, Wan Q, et al. Detection and Identification of Peroxiredoxin 3 as a Biomarker in Hepatocellular Carcinoma by a Proteomic Approach. *Int J Mol Med* (2012) 29(5):832–40. doi: 10.3892/ijmm.2012.916
55. Khayyat A, Tobwala S, Hart M, Ercal N. N-Acetylcysteine Amide, a Promising Antidote for Acetaminophen Toxicity. *Toxicol Lett* (2016) 241:133–42. doi: 10.1016/j.toxlet.2015.11.008
56. Fisher ES, Curry SC. Evaluation and Treatment of Acetaminophen Toxicity. *Adv Pharmacol* (2019) 85:263–72. doi: 10.1016/bs.apha.2018.12.004
57. Phillips AJ, Littlejohn J, Yewdall NA, Zhu T, Valéry C, Pearce FG, et al. Peroxiredoxin is a Versatile Self-Assembling Tecton for Protein Nanotechnology. *Biomacromolecules* (2014) 15(5):1871–81. doi: 10.1021/bm500261u

Conflict of Interest: The authors declare that the research was conducted in the absence of any commercial or financial relationships that could be construed as a potential conflict of interest.

Copyright © 2021 Wang, Zhao, Wang, Sun, Zou, Li, Liu, Lin, Zhou, Ning, Tian and Yao. This is an open-access article distributed under the terms of the Creative Commons Attribution License (CC BY). The use, distribution or reproduction in other forums is permitted, provided the original author(s) and the copyright owner(s) are credited and that the original publication in this journal is cited, in accordance with accepted academic practice. No use, distribution or reproduction is permitted which does not comply with these terms.